J. Fluid Mech. (1965), *vol.* 23, *part* 4, *pp.* 749–766
Printed in Great Britain

The velocity of rise of distorted gas bubbles in a liquid of small viscosity

By D. W. MOORE
Goddard Institute for Space Studies, New York City

(Received 21 January 1965)

The terminal velocity of rise of small, distorted gas bubbles in a liquid of small viscosity is calculated. Small viscosity means that the dimensionless group $g\mu^4/\rho T^3$, where g is the acceleration of gravity, μ the viscosity, ρ the density and T the surface tension, is less than 10^{-8}. It is assumed—and the numerical accuracy of the assumption is discussed—that the distorted bubbles are oblate ellipsoids of revolution. The drag coefficient is found by extending the theory given recently (Moore 1963) for the boundary layer on a spherical gas bubble. The results are in reasonable quantitative agreement with the experimental data.

1. The distortion of a rising gas bubble

In a recent paper (Moore 1963, subsequently referred to as (1)) the author considered the nature of the flow set up by a spherical gas bubble rising steadily in an infinite viscous liquid. The analysis supported Levich's† (1949) contention that the flow is essentially irrotational and that the drag could be calculated from the dissipation in the irrotational flow. Rotational flow was shown to be confined to a thin boundary layer on the surface of the bubble which separated at the rear stagnation point to form a thin rotational wake. The velocity field inside the boundary layer or wake differed from that of the irrotational flow by only $O(R^{-\frac{1}{2}})$, where R is the Reynolds number, and when allowance for the boundary layer and wake was made in calculating the dissipation it was found that the drag coefficient was given by

$$C_D = \frac{48}{R}\left(1 - \frac{2{\cdot}21\ldots}{R^{\frac{1}{2}}}\right). \tag{1.1}$$

The first term on the right-hand side is Levich's original result.

It must be stressed that this picture of the flow field depends crucially on the assumption that the bubble surface cannot support any tangential stress. If the liquid contains surface active impurities, molecules of the impure substances can collect at the surface as the bubble rises, and the bubble behaves like a small solid particle. Its drag coefficient approaches that of a solid body (Haberman & Morton 1953), it has a wake like a solid body (Hartunian & Sears 1957) and its upward motion becomes unstable at a critical Reynolds number (Hartunian & Sears 1957). Thus the theory to be presented can only be applied to pure liquids

† Levich's work is described in the English translation (Levich 1962).

and, in particular, it cannot be applied to ordinary water, which always contains significant amounts of impurity (Haberman & Morton 1953).

This result was compared with the experimental data of Haberman & Morton (1953) and, while reasonable agreement was achieved, it was pointed out that at $R = O(10^2)$ gas bubbles, in all liquids for which data are available, show significant deviation from the spherical. Thus a really decisive test of the theory was not possible. The purpose of this paper is to extend the theory to distorted bubbles.

In (1) it is shown that the normal stress at the bubble surface is equal to the pressure in the irrotational flow plus correction terms which are $O(R^{-1})$ and which arise from the normal viscous stress, the correction to the pressure due to the boundary layer and to gravity. Thus one has to determine a surface S such that

$$p + T\{(1/R_1) + (1/R_2)\} = p_{\text{gas}} \tag{1.2}$$

on S, where p is the pressure in the irrotational flow past S, $(1/R_1) + (1/R_2)$ the total curvature of S, and T the surface tension. The fact that at large Reynolds numbers the shape is independent of viscous mechanics (though, of course, it depends on the viscosity since the terminal velocity does) greatly simplifies the problem. However, the resulting inviscid free-boundary problem is very difficult and only approximate solutions are available. If the distortion is small it is a simple matter to show (Moore 1959) that the bubble is an oblate spheroid and that the ratio of the cross-stream axis, to the parallel axis, χ, is given by

$$\chi = 1 + \tfrac{9}{64} W + O(W^2), \tag{1.3}$$

where

$$W = 2r_e \rho U^2 / T \tag{1.4}$$

is the Weber number, r_e is the radius of the sphere of the same volume as the bubble, ρ is the liquid density and U is the speed of rise. W is clearly the ratio of the dynamic pressure ρU^2 causing distortion to the surface tension pressure T/r_e available to resist it.

If W is not small, the shape is unknown. It is likely, however, that for moderate values of W the bubble is still symmetric about a horizontal plane through its centre. The irrotational disturbance to a uniform stream caused by a body with fore and aft symmetry yields a symmetric pressure field on the body surface, while the total curvature is, of course, symmetric also. Moreover, this shape must be the one which continuously evolves from (1.2) as W increases. What is not certain, however, is that unsymmetric solutions do not exist to which the bubble could 'jump' at some critical W. It is well known, since the work of Davies & Taylor (1950), that bubbles at large W have a spherical-cap shape but since these bubbles are characterized by $C_D = O(1)$ it is more probable that this shape is the result of flow separation (Moore 1959; Rippin 1959).

The rest of this paper will be concerned with bubbles whose Weber number is of order unity. For such bubbles it is a fair approximation (Siemes 1954; Saffman 1956; Hartunian & Sears 1957) to assume that the bubbles are still oblate ellipsoidal. The boundary condition that the sum of the dynamic pressure and the surface tension pressure is constant on the bubble surface cannot, of course, be exactly satisfied. The simplest procedure is to satisfy the condition exactly

only at the stagnation points and at the intersection of the bubble surface and the horizontal plane of symmetry. The result is

$$W(\chi) = 4\chi^{-\frac{4}{3}}(\chi^3+\chi-2)\,[\chi^2\sec^{-1}\chi-(\chi^2-1)^{\frac{1}{2}}]^2(\chi^2-1)^{-3}. \tag{1.5}$$

The function $W(\chi)$ is plotted in figure 1. It is striking that the function has a maximum at $\chi \doteqdot 6{\cdot}0$, suggesting that there is a maximum Weber number of 3·745... above which the symmetric shape is impossible. For a given Weber number less than 3·745... the more distorted shape is, probably, unstable and will not occur in practice. It is, of course, possible that this limitation on the Weber number for symmetric bubbles is a property of the approximation, which is, as will shortly be shown, rather poor if $\chi > 2$. It would be interesting to know

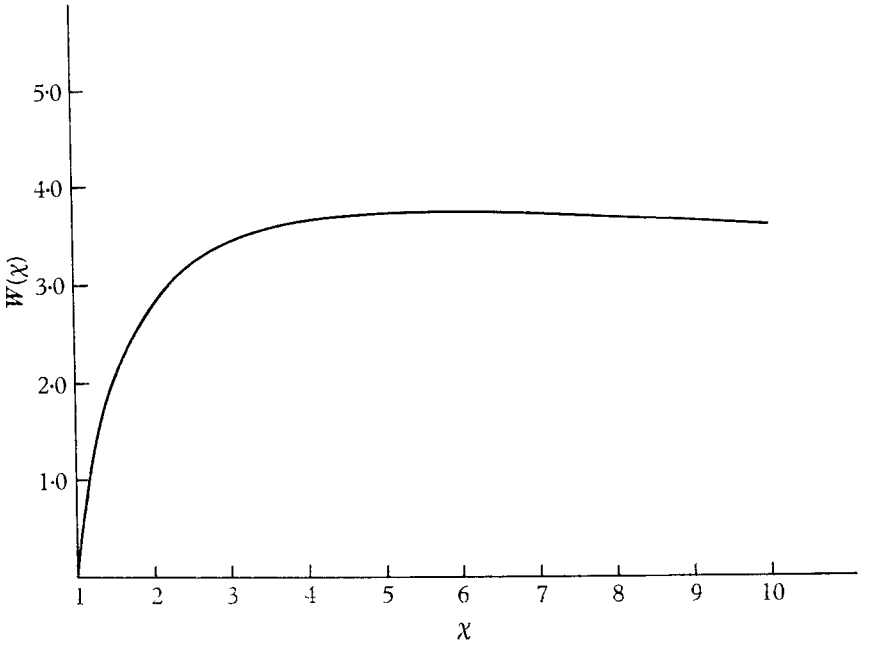

FIGURE 1. The function $W(\chi)$.

if, in the exact theory, symmetric solutions exist only below a critical Weber number. There is evidence from the drag curves of Haberman & Morton (1953) of a change of flow pattern at $W \doteqdot 4$, but this could equally be due to instability. Both Saffman (1956) and Hartunian & Sears (1957) found that instabilities could occur in this Weber number range.

The accuracy of (1.5) can be investigated numerically. It can be shown that (1.5) reduces to a form equivalent to (1.3) as $\chi \to 1$, but for larger values of χ the quantity on the left-hand side of (1.2) will not be constant on the surface of the assumed ellipsoid and will vary from its common value at the stagnation points and equator. A convenient measure of the error is the fractional change in total curvature which would be necessary to make the left-hand side, evaluated at a general point of the bubble surface, equal to the stagnation and equatorial value. Calculation showed that for $\chi = 2$ the maximum change was 10%, for

$\chi = 3$, 30 % and, for $\chi = 4$, 55 %. Thus the approximation is reasonable at $\chi = 2$, but is unreliable at $\chi = 4$.

It is clearly essential to estimate the order of magnitude of the Reynolds number at which significant distortion starts. If it should turn out that, for a particular liquid, significant distortion, which can arbitrarily be taken to be $\chi \geqslant 1{\cdot}05$,† should occur at low Reynolds numbers, then the considerations of this paper could not be applied: the bubbles would be extremely distorted when the Reynolds number was sufficiently large for boundary-layer theory to apply, and the approximation of ellipsoidal shape would be invalid. Now it follows from Levich's result that

$$U \cong g\rho r_e^2/9\mu \tag{1.6}$$

for spherical bubbles at large Reynolds numbers. Hence, using (1.3),

$$\chi - 1 = 0{\cdot}043 R^{\frac{4}{3}} M^{\frac{1}{3}},$$

where

$$M = g\mu^4/\rho T^3 \tag{1.7}$$

is a dimensionless group introduced by Haberman & Morton (1953) and also by Peebles & Garber (1953) (who call it G_1). Thus 5 % distortion occurs when

$$R = 1{\cdot}1 M^{-\frac{1}{8}}. \tag{1.8}$$

For thick liquids, such as oils, M is $O(10^{-2})$, while for a large class of 'thin' liquids, including water and many volatile organic liquids, M is $O(10^{-10})$. For high M liquids distortion sets in at low Reynolds numbers (Taylor & Acrivos 1964), while for low M liquids distortion is delayed until $R = O(10^2)$. Thus the theory presented in subsequent sections will be restricted to low M liquids.

In § 2 Levich's result is extended to the ellipsoidal bubble. It is found that the drag coefficient rises very steeply with the axis ratio χ.

It has been seen that distortion will become important at Reynolds numbers of about 100, and at these Reynolds numbers the correction to Levich's result calculated in (**1**) and which is displayed in (1.1) cannot be neglected. To find this correction the structure of the boundary layer and wake for an ellipsoidal bubble must be determined. This involves lengthy algebra which is summarized in §§ 3 and 4, but the principle of the calculation and its justification in terms of the viscous mechanics of the boundary layer are identical with those of the spherical case and the reader is referred to (**1**) for the relevant fluid-mechanical analysis.

The dependence of the correction on the axis ratio is very strong and is in the direction of increasing the drag coefficient as the axis ratio is increased. Thus the leading terms of the Reynolds number expansion of C_D both increase rapidly with the distortion, resulting in a minimum in the curve of C_D versus R.

In § 5 the experimental data on low M liquids is described and a detailed comparison of theory and experiment is attempted for three low M liquids. The agreement is quite reasonable in view of the approximations made in the shape.

The calculations of §§ 1 and 2 parallel an earlier calculation of Siemes (1954), who also considered the dissipation in the potential flow around a distorted

† This will correspond to about a 6 % increase in the drag and a 3 % decrease in the speed of rise according to the theory of §§ 2 and 3.

bubble, the bubble being approximately represented by an oblate spheroid. There are, however, small numerical differences due to a minor algebraic error in Siemes's calculation of the dissipation, so that it was felt to be worth while to repeat the calculation in detail. Siemes did not discuss the boundary layer, but his results are qualitatively similar and, in particular, he also finds a minimum in the curve of drag coefficient against Reynolds number.

2. A first approximation to the drag

Adopt rectangular axes OX, OY, OZ with O at the centre of the bubble and OZ parallel to and in the same sense as the undisturbed flow. Then the surface of the bubble is represented by the equation

$$\frac{x^2+y^2}{c^2}+\frac{z^2}{a^2}=1, \tag{2.1}$$

where $c \geqslant a$. The discussion of the potential flow past this oblate ellipsoid of revolution is best carried out in orthogonal co-ordinates (α, β, ϕ) defined by

$$\left.\begin{aligned} x &= \kappa[(1+\alpha^2)(1-\beta^2)]^{\frac{1}{2}}\cos\phi, \\ y &= \kappa[(1+\alpha^2)(1-\beta^2)]^{\frac{1}{2}}\sin\phi, \\ z &= \kappa\alpha\beta. \end{aligned}\right\} \tag{2.2}$$

Then the line elements h_1, h_2, h_3, defined by

$$dx^2+dy^2+dz^2 = h_1^2 d\alpha^2 + h_2^2 d\beta^2 + h_3^2 d\phi^2,$$

are given by

$$h_1 = \kappa\left(\frac{\alpha^2+\beta^2}{1+\alpha^2}\right)^{\frac{1}{2}}, \quad h_2 = \kappa\left(\frac{\alpha^2+\beta^2}{1-\beta^2}\right)^{\frac{1}{2}}, \quad h_3 = \kappa[(1+\alpha^2)(1-\beta^2)]^{\frac{1}{2}}. \tag{2.3}$$

One can readily verify that the surface $\alpha = \alpha_0$ coincides with (2.1) provided that

$$\kappa(1+\alpha_0^2)^{\frac{1}{2}} = c, \quad \kappa\alpha_0 = a. \tag{2.4}$$

It is most convenient to work in a frame in which the bubble is at rest. Then if the speed of the undisturbed stream is U the irrotational velocity field is grad $\overline{\phi}$ where the velocity potential $\overline{\phi}$ is given by

$$\overline{\phi} = U\kappa\{\alpha\beta + p\beta(1-\alpha\cot^{-1}\alpha)\}, \tag{2.5}$$

and where

$$p(\alpha_0) = [\cot^{-1}\alpha_0 - \alpha_0/(1+\alpha_0^2)]^{-1}. \tag{2.6}$$

This result is derived by Lamb (1932, p. 144). As in (**1**), an overbar denotes the irrotational flow past the bubble.

The dissipation $\bar{\Phi}$ in this potential flow must now be calculated. The dissipation can be expressed as an integral, over the body surface S, of the normal gradient of the square of the fluid speed (Lamb 1932, p. 581), but a more convenient result, which is easily established, is that

$$\bar{\Phi} = -2\mu\int_S \overline{u}_j \bar{e}_{ij} l_i \, dS, \tag{2.7}$$

where $\bar{\mathbf{u}}$ is the potential flow, $\bar{e}_{ij}$ is the rate of strain tensor

$$\tfrac{1}{2}(\partial\overline{u}_i/\partial x_j + \partial\overline{u}_j/\partial x_i)$$

and $\mathbf{l}$ is the normal to S drawn into the fluid.

This result has a simple physical significance. Suppose that S is made up of a large number of small rollers and that these rollers are adjusted so that they exert a force $-2\mu\bar{e}_{ij}l_i$ on the fluid, where $\bar{u}_j$ is the irrotational flow past S. Then $\bar{u}_j$ is clearly the exact solution of the full Navier–Stokes equations and (2.7) emerges as the condition that all the work done on the fluid by the rollers is dissipated by viscosity.

In the present case this surface integral becomes

$$\bar{\Phi} = -2\mu \int_{\alpha=\alpha_0} \bar{q}_\beta \bar{e}_{\alpha\beta}\, dS.\dagger$$

Now
$$(\bar{q}_\beta)_{\alpha=\alpha_0} = U\left(\frac{1-\beta^2}{\alpha_0^2+\beta^2}\right)^{\frac{1}{2}} \frac{p}{1+\alpha_0^2},$$

and
$$(\bar{e}_{\alpha\beta})_{\alpha=\alpha_0} = \frac{1}{2}\left[\frac{h_2}{h_1}\frac{\partial}{\partial\alpha}\left(\frac{\bar{q}_\beta}{h_2}\right)+\frac{h_1}{h_2}\frac{\partial}{\partial\beta}\left(\frac{\bar{q}_\alpha}{h_1}\right)\right]_{\alpha=\alpha_0}$$

so that, recalling that $\bar{q}_\alpha = 0$ on $\alpha = \alpha_0$ for all β, one finds

$$(\bar{e}_{\alpha\beta})_{\alpha=\alpha_0} = -\frac{U\alpha_0 p}{\kappa}\left(\frac{1-\beta^2}{1+\alpha_0^2}\right)^{\frac{1}{2}} \frac{1}{(\alpha_0^2+\beta^2)^2}, \tag{2.8}$$

while, finally,

$$dS = 2\pi\kappa^2(1+\alpha_0^2)^{\frac{1}{2}}(\alpha_0^2+\beta^2)^{\frac{1}{2}}\, d\beta.$$

Substituting and performing the integration one finds that

$$\bar{\Phi} = \frac{4\mu\pi U^2\kappa p^2}{(1+\alpha_0^2)}\left\{\frac{1}{\alpha_0}+\frac{1-\alpha_0^2}{\alpha_0^2}\cot^{-1}\alpha_0\right\}. \tag{2.9}$$

This calculation was attempted by Siemes (1954) but, unfortunately, a minor algebraic slip was made. In fact, the numerical effect of this error is rather small and, in the range of bubble shapes examined by Siemes, amounts only to a few per cent.

The drag on the bubble can now be found and on introducing a drag coefficient C_D defined by

$$\text{Drag} = \tfrac{1}{2}\rho U^2 \pi r_e^2 C_D,\ddagger \tag{2.10}$$

one finds
$$C_D = (48/R)\, G(\chi), \tag{2.11}$$

where

$$G(\chi) = \tfrac{1}{3}\chi^{\frac{4}{3}}(\chi^2-1)^{\frac{3}{2}}[(\chi^2-1)^{\frac{1}{2}}-(2-\chi^2)\sec^{-1}\chi]/[\chi^2\sec^{-1}\chi-(\chi^2-1)^{\frac{1}{2}}]^2, \tag{2.12}$$

and where the Reynolds number R is defined by

$$R = 2r_e U\rho/\mu \tag{2.13}$$

(χ is the axis ratio c/a).

† The velocity components in the oblate-ellipsoidal co-ordinates are written $(q_\alpha, q_\beta, 0)$.

‡ It should be noted that πr_e^2 is not the projected area on a plane perpendicular to the flow direction as is strictly required by aerodynamic usage. The reason is that r_e is what is measured experimentally—the actual projected area involves a difficult measurement of shape, so that most experimental workers adhere to the definition (2.10).

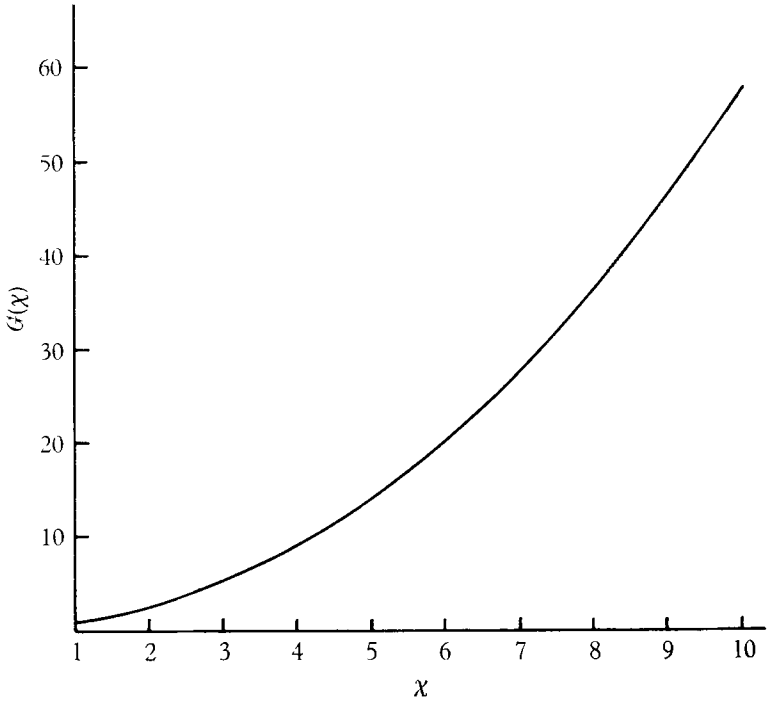

FIGURE 2. The function $G(\chi)$.

Figure 2 shows how $G(\chi)$ varies with χ. For $\chi = 1$, $G = 1$, corresponding to the spherical bubble. As χ increases $G(\chi)$ increases rapidly, showing that a bubble of given volume will experience an increased drag, and will thus rise more slowly, due to the distortion of its surface.

This result is asymptotically correct as $R \to \infty$. For liquids in which significant distortion does not occur until very large Reynolds numbers, no further calculations are necessary since, for such liquids, the results for the spherical bubble can be used for smaller values of R. One can characterize such liquids by finding the order of magnitude of M for which the boundary-layer correction to (2.11) becomes negligible while the bubble is still spherical. The analysis of § 1 shows that the condition is simply

$$2M^{\frac{1}{10}} \ll 1. \tag{2.14}$$

As far as the author is aware, there are no liquids at all for which (2.14) is strictly satisfied! However, there are some liquids† with $M = O(10^{-12})$ (so that $2M^{\frac{1}{10}}$ is about 0·13) for which (2.11) and (1.1) would provide a fair approximation to the drag coefficient over a whole range of large Reynolds numbers—unfortunately, there are not very many experimental data on these very low M liquids.‡

Thus the boundary-layer correction to (2.11) must be sought and in the next two sections of this paper the calculations are described.

† Their existence was pointed out to the author by Dr J. F. Harper and a list of low M liquids he compiled is given in the appendix.

‡ Peebles & Garber (1953) give a few measurements on acetone.

3. The boundary-layer equations and their solutions

The irrotational solution $\overline{\phi}$ satisfies all the boundary conditions of the problem except the vanishing of the tangential stress at the surface of the bubble. As was argued in detail in (**1**) this implies that there will, at high Reynolds numbers, be a thin boundary layer at the bubble surface in which the velocity field changes by $O(R^{-\frac{1}{2}})$ whilst the stress field changes by $O(R^{-1})$ to annul to $O(R^{-1})$ surface stress corresponding to the potential solution. The purpose of this section is to derive the equations governing this boundary layer.

If $\mathbf{u}'$ is the actual velocity field and p' the pressure, the steady-state Navier–Stokes equations are

$$-\mathbf{u}' \wedge \operatorname{curl} \mathbf{u}' = -\nabla(p'/\rho + \tfrac{1}{2}\mathbf{u}'^2) + \nu\nabla^2\mathbf{u}', \quad \operatorname{div} \mathbf{u}' = 0. \tag{3.1}$$

If one introduces the substitutions

$$\mathbf{u}' = \bar{\mathbf{u}} + \mathbf{u}, \quad p' = \bar{p} + p, \tag{3.2}$$

into (3.1) and neglects quadratic terms in $\mathbf{u}$ one finds that

$$-\bar{\mathbf{u}} \wedge \operatorname{curl} \mathbf{u} = -\nabla(p/\rho + \bar{\mathbf{u}} \cdot \mathbf{u}) + \nu\nabla^2\mathbf{u}, \quad \operatorname{div} \mathbf{u} = 0. \tag{3.3}$$

One can now express (3.3) in terms of the co-ordinates α, β and make the usual boundary-layer approximations symbolized by $\partial/\partial\alpha \gg \partial/\partial\beta$ and $q_\alpha \ll q_\beta$. The α-component of the momentum equation shows that the pressure perturbation is only $O(R^{-1})$ in the boundary layer so that the β component of the momentum equation becomes

$$\bar{q}_\alpha \frac{1}{\bar{h}_1^0}\frac{\partial q_\beta}{\partial\alpha} + \frac{1}{\bar{h}_2^0}\frac{\partial}{\partial\beta}(\bar{q}_\beta q_\beta) = \frac{\nu}{(\bar{h}_1^0)^2}\frac{\partial^2 q_\beta}{\partial\alpha^2}, \tag{3.4}$$

where the zero attached to the line elements indicates that they are to be evaluated at $\alpha = \alpha_0$. One recalls that $\bar{q}_\alpha = O(\alpha - \alpha_0)$ in the boundary layer so that the two terms on the left-hand side of (3.4) are of the same order of magnitude.

The boundary conditions are

$$q_\beta = 0 \quad \text{on} \quad \beta = -1, \quad \text{all } \alpha, \tag{3.5}$$

$$q_\beta \to 0 \quad \text{as} \quad \alpha \to \infty, \quad -1 \leqslant \beta \leqslant 1, \tag{3.6}$$

$$\frac{1}{2\bar{h}_1^0}\frac{\partial q_\beta}{\partial\alpha} + \bar{e}_{\alpha\beta} = 0 \quad \text{on} \quad \alpha = \alpha_0, \quad -1 \leqslant \beta \leqslant 1. \tag{3.7}$$

The last condition insists that the tangential surface stress is zero.

The process leading to (3.4) and, in particular, the orders of magnitude of the non-linear terms were examined in (**1**) for the special case of the spherical bubble. There seems no reason to anticipate any difference in the behaviour of the neglected terms in the present case, so that the argument given in (**1**) to justify the process will not be repeated.

If the explicit expressions for $\bar{q}_\alpha$, $\bar{q}_\beta$ and $\bar{e}_{\alpha\beta}$ are introduced one finds, after some algebra, that the boundary-layer equation is

$$\frac{3y'\beta}{(\alpha_0^2+\beta^2)}\frac{\partial u}{\partial y'} + \left(\frac{1-\beta^2}{\alpha_0^2+\beta^2}\right)^{\frac{1}{2}}\frac{\partial}{\partial\beta}\left[\frac{3}{2}\left(\frac{1-\beta^2}{\alpha_0^2+\beta^2}\right)^{\frac{1}{2}}u\right] = \frac{1}{\alpha_0^2+\beta^2}\frac{\partial^2 u}{\partial y'^2}, \tag{3.8}$$

with boundary conditions

$$u = 0 \quad \text{on} \quad \beta = -1, \quad \text{all } y', \tag{3.9}$$

$$u \to 0 \quad \text{as} \quad y' \to \infty, \quad -1 \leqslant \beta \leqslant +1, \tag{3.10}$$

$$\frac{\partial u}{\partial y'} = \frac{3(1-\beta^2)^{\frac{1}{2}}}{(\alpha_0^2+\beta^2)^{\frac{3}{2}}}\,\alpha_0^2 \quad \text{on} \quad y' = 0, \quad -1 \leqslant \beta \leqslant 1, \tag{3.11}$$

where for convenience dimensionless quantities are introduced according to the scheme

$$\left.\begin{aligned} q_\beta &= \hat{U}\,\delta u, \quad y' = (\alpha - \alpha_0)\,\delta^{-1}, \\ \text{where} \qquad \hat{U} &= \frac{2}{3}\,\frac{Up}{\alpha_0(\alpha_0^2+1)}, \quad \text{and} \quad \delta = \left[\frac{\nu(1+\alpha_0^2)}{\kappa\alpha_0\,\hat{U}}\right]^{\frac{1}{2}}; \end{aligned}\right\} \tag{3.12}$$

y' is a dimensionless boundary-layer normal co-ordinate. The problem just posed can be solved by transforming (3.8) into the heat-conduction equation. The transformations

$$\left.\begin{aligned} X &= \tfrac{2}{9}(\beta+1)^2(2-\beta), \quad Y = (1-\beta^2)\,y', \\ u(\beta, y') &= [(\alpha_0^2+\beta^2)/(1-\beta^2)]^{\frac{1}{2}}\,v(X, Y) \end{aligned}\right\} \tag{3.13}$$

accomplish this and one is left with the problem

$$\partial v/\partial X = \partial^2 v/\partial Y^2, \tag{3.14}$$

$$v = 0 \quad \text{on} \quad X = 0, \tag{3.15}$$

$$v \to 0 \quad \text{as} \quad Y \to \infty, \qquad X > 0, \tag{3.16}$$

$$\partial v/\partial Y = 3\alpha_0^2/\{\alpha_0^2+\beta^2(X)\}^2 = S(X), \quad \text{say,} \quad \text{on } Y = 0, \tag{3.17}$$

whose solution,

$$\frac{\partial v}{\partial Y} = \frac{Y}{2\sqrt{\pi}}\int_0^X \frac{S(\tau)}{(X-\tau)^{\frac{3}{2}}}\exp\left[-\frac{Y^2}{4(X-\tau)}\right]d\tau, \tag{3.18}$$

is immediate (Carslaw & Jaeger 1959, p. 295). This gives finally

$$v = -\frac{1}{\sqrt{\pi}}\int_0^X \frac{S(\tau)}{(X-\tau)^{\frac{1}{2}}}\exp\left[-\frac{Y^2}{4(X-\tau)}\right]d\tau. \tag{3.19}$$

One must examine how $u(\beta, y')$ behaves as $\beta \to -1$ and $\beta \to +1$, that is to say as the front and rear stagnation points are approached. If $\beta \to -1+0$, (3.13) shows that

$$u(\beta, y') \sim \frac{(\alpha_0^2+1)}{\sqrt{2}(1+\beta)^{\frac{1}{2}}}\,v(X, Y) = \frac{\alpha_0^2+1}{\sqrt{3}\,X^{\frac{1}{4}}}\,v(X, Y).$$

Now from (3.19)

$$v = O(X^{\frac{1}{2}}) \quad \text{as} \quad X \to 0+,$$

so that

$$u = O(X^{\frac{1}{4}}) \quad \text{as} \quad X \to 0+.$$

Thus u is regular near the front stagnation point and vanishes on the axis of symmetry. However, as $\beta \to 1-0$, $X \to \frac{8}{9}$ and so $v(X, Y)$ remains finite. Thus (3.13) shows that $u(\beta, Y) \to \infty$ so that, just as for the spherical bubble, the boundary-layer solution has a singularity at the rear stagnation point.

Clearly the boundary-layer solution fails near the rear stagnation point and there will be a region in which the flow separates from the bubble and joins on to the wake. The nature of this separation in the spherical case was examined in (1) and it was concluded that (*A*) viscous forces are negligible in this region—large inertia forces are introduced by the rapid turning while, at the same time, the viscous stresses are reduced by the thickening of the boundary layer; (*B*) the total velocity field is still only slightly perturbed from the irrotational velocity field $\bar{u}$. (*A*) and (*B*) mean that the vorticity, ω, satisfies

$$\omega/m = B(\overline{\psi}), \tag{3.20}$$

where, as in (1), m denotes the distance from the axis. Also (*C*) there is a region of overlap in which the boundary-layer solution is still valid but viscous forces can be neglected. (*C*) means that $B(\overline{\psi})$ can be determined by matching.

The structure of the wake and hence the contribution of the wake to the viscous dissipation will depend on $B(\overline{\psi})$, so that the next step is to determine this function.

4. The dissipation

The vorticity in the boundary layer is

$$\omega = \frac{1}{h_1^0}\frac{\partial q_\beta}{\partial \alpha},$$

and in terms of the transformed variables this is, for $\beta \to 1-$,

$$\omega = (\hat{U}/\kappa)(1+\alpha_0^2)^{\frac{1}{2}}(2\eta)^{\frac{1}{2}}\,\partial v/\partial Y,$$

where $\eta = 1-\beta$, and it has been assumed that $\eta \ll 1$. To the same order of approximation

$$m = \kappa(1+\alpha_0^2)^{\frac{1}{2}}(2\eta)^{\frac{1}{2}},$$

so that
$$\frac{\omega}{m} = \frac{\hat{U}}{\kappa^2}\frac{\partial v}{\partial Y} = \frac{\hat{U}}{\kappa^2}\frac{Y}{2\sqrt{\pi}}\int_0^{\frac{8}{9}} \frac{S(\tau)}{(\frac{8}{9}-\tau)^{\frac{3}{2}}}\exp[-Y^2/4(\tfrac{8}{9}-\tau)]\,d\tau. \tag{4.1}$$

Now
$$\overline{\psi} = \tfrac{1}{2}U\kappa^2(1+\alpha^2)(1-\beta^2)\{1+p(\alpha/(1+\alpha^2)-\cot^{-1}\alpha)\},$$

and if one assumes that $1-\beta$ and $\alpha-\alpha_0$ are small one finds that

$$\overline{\psi} = \tfrac{3}{2}\delta\alpha_0\,\hat{U}\kappa^2 Y = Y/2f, \quad \text{say.} \tag{4.2}$$

One is now in a position to see that (4.1) confirms that $\omega/m = B(\overline{\psi})$, and that

$$B(\overline{\psi}) = \frac{\hat{U}}{\kappa^2}\frac{f\overline{\psi}}{\sqrt{\pi}}\int_0^{\frac{8}{9}} \frac{S(\tau)}{(\frac{8}{9}-\tau)^{\frac{3}{2}}}\exp[-f^2\overline{\psi}^2/(\tfrac{8}{9}-\tau)]\,d\tau. \tag{4.3}$$

The structure of the wake behind a spherical gas bubble was discussed in some detail in (1). It was shown that the wake was of breadth $O(R^{-\frac{1}{4}})$ and that the perturbation of the irrotational flow was $O(R^{-\frac{1}{2}})$ in the wake. Viscous forces were small and produced no significant modification to the velocity profile until the distance downstream from the bubble was $O(R^{\frac{1}{2}})$. This last remark is important since it means that there is a region where the wake is essentially a parallel flow whilst still being determined by inviscid mechanics.

Thus, in this region, the velocity is easily determined. The vorticity in the wake is $\partial q_z/\partial m$, where q_z is the axial velocity component and $\overline{\psi} = \frac{1}{2}Um^2$ so that (3.20) gives

$$\partial q_z/\partial m = mB(\tfrac{1}{2}Um^2), \tag{4.4}$$

and, since $q_z \to 0$ as $m \to \infty$, q_z is completely determined.

One is now in a position to calculate the dissipation in the wake. However, (4.4) will first be used to find the momentum defect associated with the wake. The comparison of the drag found in this way with that obtained in § 2 will provide a partial check on the validity of (3.18).

The pressure is negligible in the wake so that the analysis of § 4 of (**1**) shows that the drag D is given by

$$D = -\rho U \int_0^\infty 2\pi m q_z \, dm.$$

The distance from the axis m can be replaced by $\overline{\psi}$ and after a partial integration

$$D = 2\pi\rho \int_0^\infty \overline{\psi} \frac{\partial q_z}{\partial \overline{\psi}} d\overline{\psi},$$

so that, using (4.4),

$$D = \frac{2\pi\rho}{U} \int_0^\infty \overline{\psi} B(\overline{\psi}) \, d\overline{\psi}.$$

Thus

$$D = \frac{2\pi\rho\hat{U}f}{U\kappa^2\sqrt{\pi}} \int_0^\infty \overline{\psi}^2 \int_0^{\frac{8}{9}} \frac{S(\tau)}{(\frac{8}{9}-\tau)^{\frac{3}{2}}} \exp\left[-f^2\overline{\psi}^2/(\tfrac{8}{9}-\tau)\right] d\tau \, d\overline{\psi},$$

and on inverting the order of integration and carrying out one integration,

$$D = \frac{\pi\rho\hat{U}}{2\kappa^2 U f^2} \int_0^{\frac{8}{9}} S(\tau) \, d\tau.$$

If one substitutes for $S(\tau)$ from (3.17) and changes the variables, one has

$$D = \frac{\pi\rho\hat{U}}{\kappa^2 U f^2} \alpha_0^2 \int_{-1}^{+1} \frac{(1-\beta^2)}{(\alpha_0^2+\beta^2)^2} d\beta,$$

and it is now a simple matter to substitute for $\hat{U}$ and f using (3.12) and (4.2) and confirm that D agrees with the value given in § 2.

The dissipation associated with the boundary layer and with the wake may now be calculated. The contribution from the boundary layer is expressed, as in (**1**), by a volume integral and a surface integral, whilst the contribution from the wake is reduced to a surface integral over a cross-section of the wake.

Tedious but straightforward manipulations now show that the net dissipation from the boundary layer and wake is Φ, where

$$\Phi = \mu\hat{U}^2 \delta\kappa(1+\alpha_0^2)\sqrt{\pi}[I_1(\alpha_0) - 12\alpha_0^2 I_2(\alpha_0) + \tfrac{3}{2}p^2 I_3(\alpha_0)/(\alpha_0^2+1)^2], \tag{4.5}$$

with

$$\left.\begin{aligned} I_1(\alpha_0) &= \int_{-1}^{+1} (\alpha_0^2+\beta^2)\, d\beta \int_0^{X(\beta)} \int_0^{X(\beta)} \frac{S(\tau)S(\tau')}{(2X-\tau-\tau')^{\frac{3}{2}}} d\tau \, d\tau', \\ I_2(\alpha_0) &= \int_{-1}^{+1} \frac{d\beta}{(\alpha_0^2+\beta^2)} \int_0^{X(\beta)} \frac{S(\tau)\, d\tau}{(X-\tau)^{\frac{1}{2}}}, \\ \text{and} \quad I_3(\alpha_0) &= \int_0^{\frac{8}{9}} \int_0^{\frac{8}{9}} \frac{S(\tau)S(\tau')}{(\frac{16}{9}-\tau-\tau')^{\frac{1}{2}}} d\tau \, d\tau'. \end{aligned}\right\} \tag{4.6}$$

The integrals I_1, I_2, and I_3 arise from the volume integral through the boundary layer, the surface integral over the bubble surface and the surface integral over a cross-section of the wake, respectively. They cannot usefully be reduced because of the complexity of $S(\tau)$.

One can finally write

$$C_D = \frac{48}{R} G(\chi) \left\{1 + \frac{H(\chi)}{R^{\frac{1}{2}}} + o\left(\frac{1}{R^{\frac{1}{2}}}\right)\right\}, \tag{4.7}$$

where $H(\chi)$ has to be obtained by numerical integration, although one can verify analytically that

$$H(\chi) \to -4\sqrt{2}(6\sqrt{3} + 5\sqrt{2} - 14)/5\sqrt{\pi} \quad \text{as} \quad \chi \to 1, \tag{4.8}$$

in agreement with the result for a spherical bubble. The function $H(\chi)$ is given in table 1 and it will be observed that it is rapidly increasing.

In § 5, (4.7) is used to calculate the velocity of rise of gas bubbles in three low M liquids for which data are available.

χ	$H(\chi)$	χ	$H(\chi)$
1·0	−2·211	2·6	+1·499
1·1	−2·129	2·7	+1·884
1·2	−2·025	2·8	+2·286
1·3	−1·899	2·9	+2·684
1·4	−1·751	3·0	+3·112
1·5	−1·583	3·1	+3·555
1·6	−1·394	3·2	+4·013
1·7	−1·186	3·3	+4·484
1·8	−0·959	3·4	+4·971
1·9	−0·714	3·5	+5·472
2·0	−0·450	3·6	+5·987
2·1	−0·168	3·7	+6·517
2·2	+0·131	3·8	+7·061
2·3	+0·448	3·9	+7·618
2·4	+0·781	4·0	+8·189
2·5	+1·131		

TABLE 1

5. Comparison with experiment

There have been two comprehensive series of experiments on the rise of small gas bubbles, those performed by Haberman & Morton (1953) and Peebles & Garber (1953). The qualitative conclusions of these workers are in agreement, but there are some puzzling quantitative differences.

In both cases, a plot of $C_D(R)$ (figures 3, 4) for all the liquids used was given and the results were qualitatively similar. $C_D(R)$ is a universal curve for all low M liquids when R is $O(10)$, but for larger R the curves start to climb away from this universal curve and then, after a minimum, rise very steeply. The drag curve would be a universal one if the bubbles remained spherical and it is plausible to invoke distortion to account for the departures. It is consistent with this interpretation that, the smaller the value of M, the larger the R at which

departures from the universal curve become apparent, since in § 1 it was shown that significant distortion should be apparent at a Reynolds number of about $M^{-\frac{1}{8}}$. The precise effect of the distortion will be discussed later.

Haberman & Morton found that, for very large R, $C_D(R)$ was a universal constant of value 2·6. Peebles & Garber did not proceed to such high Reynolds numbers

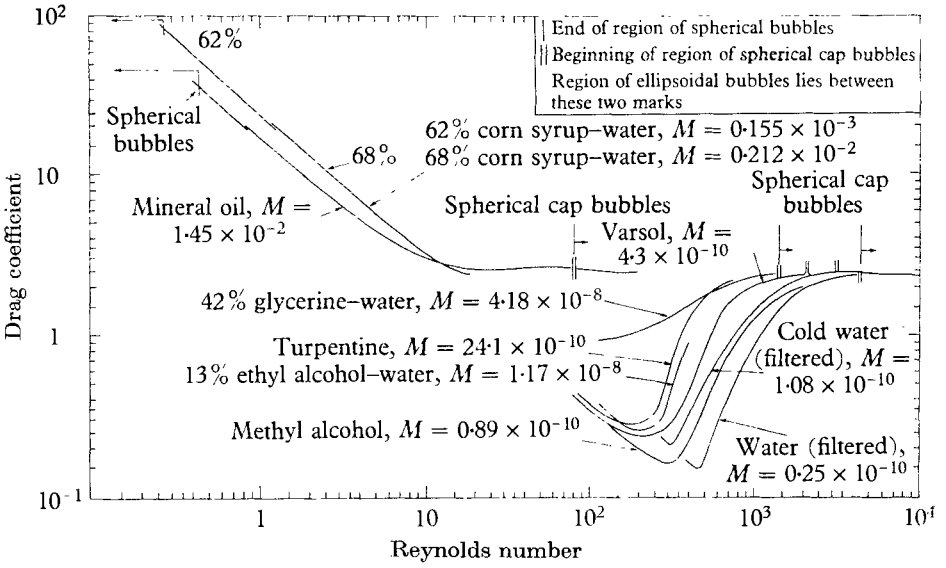

FIGURE 3. $C_D(R)$ for a number of liquids according to Haberman & Morton (1953).

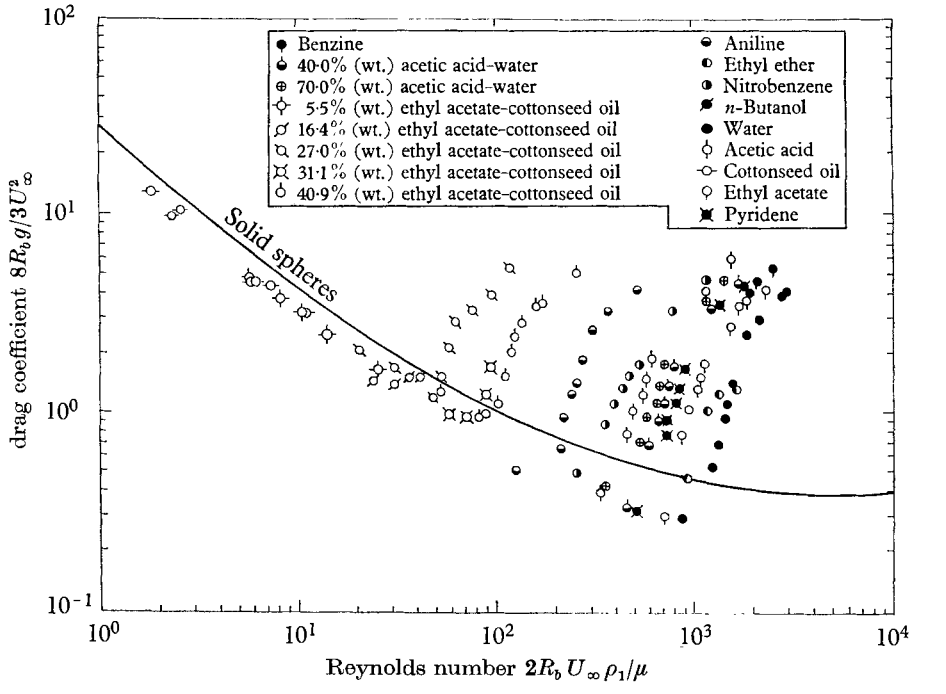

FIGURE 4. $C_D(R)$ for a number of liquids according to Peebles & Garber (1953).

and did not find this tendency. The minimum in the drag coefficient, which occurs close to the point of departure from the universal curve, and the transition to the asymptotic value for large bubbles were found by Haberman & Morton to occur at a Weber number very close to 2 for all the low M liquids they examined. Peebles & Garber did not consider $C_D(W)$ but claimed that the departure from the universal curve was at a Reynolds number given by

$$R = 4{\cdot}02M^{-0{\cdot}214}. \tag{5.1}$$

However, if we assume that the universal curve is

$$C_D = A(R)/R, \tag{5.2}$$

where $A(R)$ is slowly varying, the relation

$$C_D = \tfrac{4}{3}MR^4W^{-3}, \tag{5.3}$$

which expresses the equality of the drag force and the buoyancy in the steady state, gives

$$RM^{\frac{1}{6}} \sim W, \tag{5.4}$$

so that the results are in qualitative agreement.

Unfortunately, there is no agreement as to the actual values of C_D. Peebles & Garber give values which are about twice those found by Haberman & Morton and there does not appear to be any difference of definition or procedure to account for the discrepancy. It is not clear from their paper that Peebles & Garber made allowance for the change in bubble size under the variation of hydrostatic pressure in their test column but, in any case, the effect on the drag coefficient would be small. The only liquid common to the two series was water but it is hard to believe that there was a systematic difference between the two groups of liquids. It is well known that small amounts of surface active impurity can render the surface of the bubble effectively solid and thus increase the drag coefficient. However, although this would account for the larger values of C_D obtained by Peebles & Garber, it would not account for the internal consistency of their data. Clearly, some further work is desirable.

Both pairs of workers found that, for a given liquid, there was as the volume was increased a tendency for the bubble to rise in a helical rather than a rectilinear path. This will eventually affect the rate of rise (Saffman 1956), but it will be small for the range of bubble sizes considered here and has been ignored in the present theory.

The present theory satisfactorily accounts for the general features of the dependence of C_D on R and it is in fair quantitative agreement with Haberman & Morton's data.

It is not easy to calculate C_D for a prescribed value of R and the simplest plan is to regard the axis ratio χ as the independent variable. $W(\chi)$ is given by (1.5) and (4.7) and (5.1) enable $R(\chi)$ to be determined and thus $C_D(\chi)$ can be found. $\chi = 4$ was the largest value used. It is clear from the discussion of § 1 that the approximation to the true shape by an oblate ellipsoid is very dubious for $\chi > 2$, but it will appear from the detailed comparison that the effect of this crude approximation on the drag coefficient is less than might have been anticipated.

The variation of C_D with R for a range of values of M is shown in figure 5. It is surprising that the rapid rise of C_D after its minimum, which occurs at $W \doteqdot 1{\cdot}8$ in the theory, is predicted by a laminar theory. Such a marked rise in drag normally suggests a change in flow régime and, indeed, there is direct evidence that flow separation eventually takes place. The flow around spherical cap bubbles is certainly separated (Davies & Taylor 1950) while there is also visual evidence that the bubble surface itself becomes unstable at large Weber numbers (Hartunian & Sears 1957), which would, of course, lead to a drastic change in the flow. These effects are not denied, but the present theory suggests that care must be used in locating their onset from the drag curves.

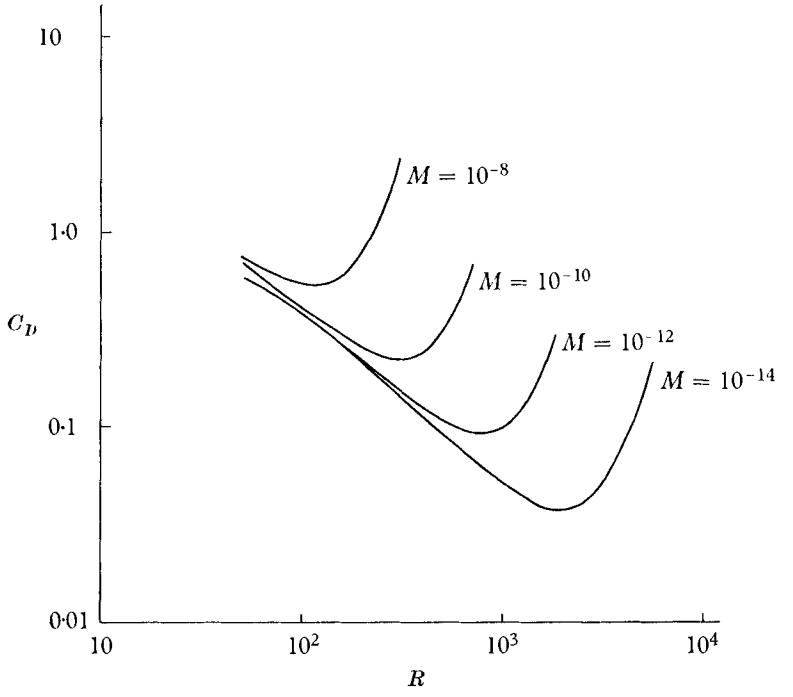

FIGURE 5. The predicted $C_D(R)$ for $M = 10^{-8}$, 10^{-10}, 10^{-12}, 10^{-14}. The right-hand end of the curves corresponds to an axis ratio χ equal to 4.

Haberman & Morton (1953) give detailed plots of U as a function of r_e for a number of liquids. They display all their experimental points, so that one can easily estimate the experimental scatter. For this reason, it is a more useful test of the theory to compare its predictions of $U(r_e)$ rather than its predictions of $C_D(R)$ or $C_D(W)$, for which Haberman & Morton give only smoothed curves.

A comparison with their experimental results for the low M liquids Varsol, turpentine and methyl alcohol is shown in figures 6–8.

The agreement is fair although the maximum velocity of rise is systematically too low. The prediction of the radius at which the velocity of rise has a maximum is too large, the discrepancy being most noticeable for methyl alcohol.

The point on the curves corresponding to $\chi = 2$ is marked A and the curves terminate at $\chi = 4$, so that an idea can be formed of the amount of distortion

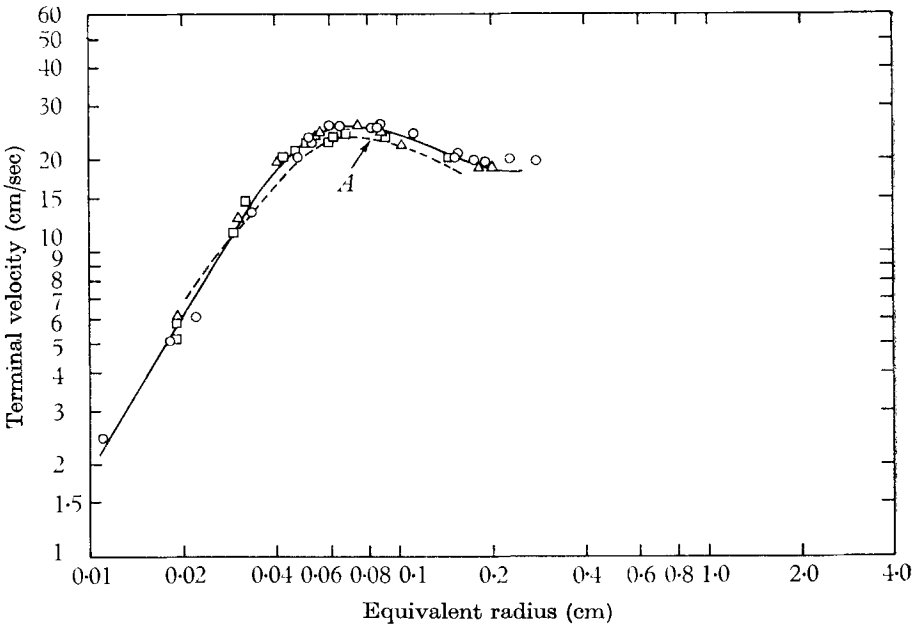

FIGURE 6. Comparison of theory and experiment for Varsol; $M = 4{\cdot}45 \times 10^{-10}$. (Haberman & Morton give $M = 4{\cdot}3 \times 10^{-10}$ and there were other small numerical discrepancies in their data on this liquid. The above value is based on the values $\mu = 8{\cdot}5 \times 10^{-3}$, $\rho = 0{\cdot}782$, $T = 24{\cdot}5$, all in c.g.s. units, which the authors give in their paper.) ----, Theory; ——, smoothed experimental curve. The three symbols denote runs in different tanks.

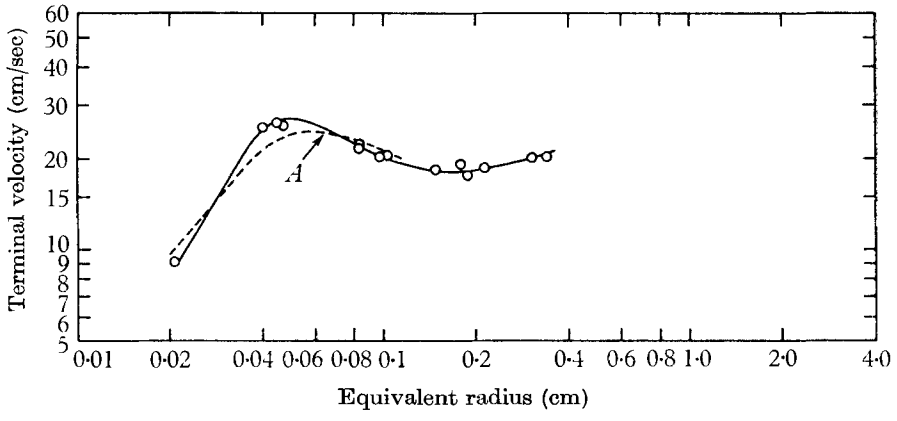

FIGURE 7. Comparison of theory and experiment for methyl alcohol; $M = 0{\cdot}89 \times 10^{-10}$. ----, Theory; ——, smoothed experimental curve.

predicted. Clearly the decreasing portion of the curve is associated with a rapid increase of distortion with r_e, resulting in a drag force which increases with r_e faster than r_e^3. It is surprising that the agreement between experiment and theory remains fair for $\chi > 2$. Unless this is fortuitous, it may mean that the drag coefficient is not very sensitive to the shape of the bubble once the axis ratio is fixed, so that the crude approximation to the shape does not matter.

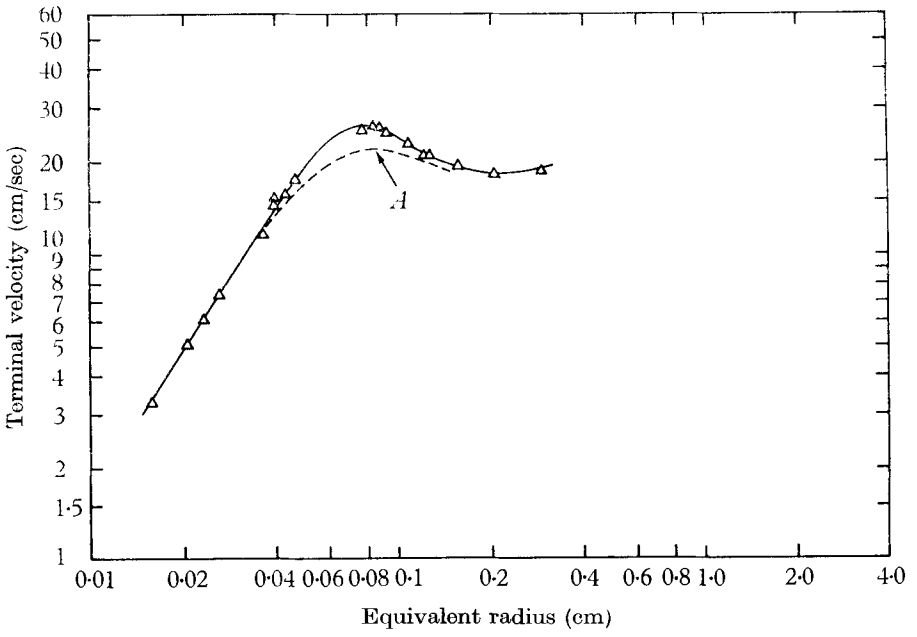

FIGURE 8. Comparison of theory and experiment for turpentine; $M = 24{\cdot}1 \times 10^{-10}$. ----, Theory; ——, smoothed experimental curve.

Most of this work was done at the University of Bristol and the author would like to thank Dr M. H. Rogers of the Computer Unit for starting the calculations. These calculations were completed by Mrs O. Ko of the Institute for Space Studies and the author would like to thank her for her invaluable assistance. He would also like to thank Dr R. Jastrow for extending to him the hospitality of the Institute for Space Studies.

REFERENCES

CARSLAW, H. S. & JAEGER, J. C. 1959 *Conduction of Heat in Solids.* Oxford: Clarendon Press.

DAVIES, R. & TAYLOR, G. I. 1950 *Proc. Roy. Soc.* A, **200**, 375.

HABERMAN, W. L. & MORTON, R. K. 1953 *David Taylor Model Basin, Rep.* no. 802.

HARTUNIAN, R. A. & SEARS, W. R. 1957 *J. Fluid Mech.* **3**, 27.

LAMB, H. 1932 *Hydrodynamics*, 6th ed. Cambridge University Press.

LEVICH, V. 1949 *Zh. Eksptl.*

LEVICH, V. 1962 *Physico-Chemical Hydrodynamics.* New York: Prentice Hall.

MOORE, D. W. 1959 *J. Fluid Mech.* **6**, 113.

MOORE, D. W. 1963 *J. Fluid Mech.* **16**, 161.

PEEBLES, F. N. & GARBER, H. J. 1953 *Chem. Engng Progr.* **49**, 88.

RIPPIN, D. W. T. 1959 Ph.D. Thesis, Cambridge University.

SAFFMAN, P. G. 1956 *J. Fluid Mech.* **1**, 249.

SIEMES, W. 1954 *Chemie-Ing.-Tech.* **26**, 614.

TAYLOR, T. D. & ACRIVOS, A. 1964 *J. Fluid Mech.* **18**, 466.

Appendix

The following list of low M liquids was prepared by Dr J. Harper from the *Handbook of Physics and Chemistry*. Data refer to 20° C. The values are approximate, due to uncertainties in T and μ.

	$M \times 10^{12}$		$M \times 10^{12}$
Acetaldehyde	3·0	Ethyl iodide	24
Acetone	11	*n*-Hexane	27
Acetonitrile	8·4	Hydrazine	11
Benzene	84	Isopentane	13
Bromine	45	Mercury	0·037
Carbon disulphide	4·0	Methyl acetate	15
Ether	8·3	Methyl alcohol†	130
Ethyl acetate	34	Methyl iodide	13
Ethyl bromide	13	Methylene chloride	14
Ethyl formate	22	*n*-Octane	120

† Haberman & Morton used methyl alcohol at 30° C, which lowers its viscosity, hence M.